6716 *Macromolecules* **2010**, *43*, 6716–6723
DOI: 10.1021/ma1009337

Macromolecules
ARTICLE

In situ Polymerization Approach to Graphene-Reinforced Nylon-6 Composites

Zhen Xu and Chao Gao*

MOE Key Laboratory of Macromolecular Synthesis and Functionalization, Department of Polymer Science and Engineering, Zhejiang University, 38 Zheda Road, Hangzhou 310027, P. R. China

Received April 28, 2010; Revised Manuscript Received July 7, 2010

ABSTRACT: We reported an efficient method to prepare nylon-6− (PA6−) graphene (NG) composites by *in situ* polymerization of caprolactam in the presence of graphene oxide (GO). During the polycondensation, GO was thermally reduced to graphene simultaneously. By adjusting the feed ratio of caprolactam to GO, various composites with 0.01−10 wt % content of graphene were obtained. The highly grafting nylon-6 arms on graphene sheets was confirmed by XPS, FTIR, TGA and AFM measurements, showing the grafting content up to 78 wt % and homogeneous 2D brush-like morphology from AFM observations. The efficient polymer-chain grafting makes the graphene homogeneously dispersed in PA6 matrix and depresses the crystallization of PA6 chains. Furthermore, we prepared NG fibers by melt spinning process, and found that the tensile strength increased by 2.1 folds and Young's modulus increased by 2.4 folds with the graphene loading of 0.1 wt % only, revealing an excellent reinforcement to composites by graphene. The *in situ* condensation polymerization approach paves the way to prepare graphene-based nanocomposites of condensation polymers with high performances and novel functionalities.

Introduction

Carbon is a common and marvelous element. Besides the well-known allotropes of graphite and diamond, other new forms of carbon have been discovered in the last few decades in succession, mainly including fullerene,[1] carbon nanotubes (CNTs),[2] and graphene.[3] Graphene, the newly discovered two-dimensional atomic carbon sheet composed of sp^2-hybridized carbon atoms in a hexagonal lattice, is considered as building blocks for other graphitic carbon of zero-dimension (0D) fullerene, 1D CNTs, and 3D graphite.[4] Because of their unique attributes respectively, different forms of graphitic carbon have been employed as fillers to prepare polymer composites with integrated properties through various methods.[5] Mechanically noncovalent mixing is a simple process for the fabrication of composites, which, however, generally resulting in poor interaction between fillers and polymer matrices.[6] To resolve this problem, either surface modification or *in situ* polymerization approach has been tried.[7] For CNTs/polymer composites, chemically functionalized CNTs have been demonstrated as efficient nanofillers for high performance composites.[8] Even though various functionalization and polymer-grafting approaches have been reported to exfoliate CNTs bundles, it is still extremely hard to access composites in which CNTs were individually dispersed in the polymer matrix due to the ultrastrong entanglement of CNTs. As to graphite/polymer composites, expanded graphite obtained by microwave treatment of graphite intercalation compounds was usually used for achieving modified dispersibility and higher interfacial interaction.[9] Although expanded graphite has been used commercially, complete exfoliation of graphite to the level of individual graphene sheets is yet to be accessed. Recently, the prosperity of graphene technology provides the successful fabrication of graphene-based composites in which graphene sheets are dispersed as individual sheets, impacting composites ascendant properties only in very low containing of graphene.[10]

*Corresponding author. E-mail: chaogao@zju.edu.cn.

Compared with other graphitic carbon, graphene possesses a vast range of unique properties and potential applications, and more attributes are to be discovered since the first individual graphene sheet fabricated using mechanical exfoliation by Geim's group.[3] The very peculiar electronic properties of graphene, representing by unprecedented carrier mobility (200 000 $cm^2/V\ s$)[11] and quantum Hall effect,[12] make graphene extraordinarily perspective as next-generation material for nanoelectronic devices. With more ascendant properties, such as high mechanical stiffness[13] and thermal conductivity[14] (1086 GPa and 3000 W $m^{-1}\ K^{-1}$ respectively), graphene either shows great potential to fabricate nanocomposites with high performances and novel functionalities for a range of applications such as electric conductive composites,[10,15,16] supercapacitors,[17] sensors,[18] biomaterials,[19] batteries,[20] ultrafast laser mode-locker,[21] and thermally stable and mechanically reinforced materials.[22,23] The manufacture of such composites of optimized performance requires that graphene sheets should be homogeneously distributed in various matrices. Similar to CNTs, pristine graphene sheets are prone to congregate in composites unfortunately for their strong $\pi-\pi$ stacking between layers and incompatible surface characteristics with the polymer matrices, posing a big obstacle for its application in nanocomposites. Therefore, chemical functionalization is needed as well to achieve the single-sheet dispersion of graphene in far-ranging polymer composites with optimum performances.

Chemical reduction of graphene oxide (GO) is one of the most addressed routes to prepare graphene on large-scale. Generally, GO is obtained by oxidation of the natural flake graphite in the presence of strong oxidants such as potassium permanganate mixed with concentrated sulfuric acid, followed by sonication.[24,25] The natural graphite flakes possess stably stacked multilayer crystalline structures with perfect sp^2-hybridized carbon atoms arranged in a honeycomb lattice in one layer and strong van der Waals forces between neighbored layers. After oxidation, abundant functional groups (e.g., hydroxyl, carboxyl,

 Published on Web 07/19/2010

epoxy, ketone, etc.) were introduced onto the graphitic layers, and simultaneously part of sp^2-carbons were converted into sp^3 ones.[25−27] Because of the strong repulsion between negative-charged layers and the enlarging of interlayer distance, the oxidized bulk graphite could be easily exfoliated into individually dispersed single layers by sonication in water. Such oxidized graphite was termed as graphene oxide (GO) recently. Because of the destruction of conjugated plane, GO is nonconductive ($\sim 10^{-4}$ S/m),[25,28] and could be reduced into single layers of conductive graphene ($\sim 10^2$ S/m)[27] for the restoring of conjugated structure.

According to the chemical structure of GO, two methodologies have been developed to covalently modify its surface with polymer on the basis of different reactive sites of carbon−carbon double bonds and functional groups, respectively. Ye and co-workers prepared amphiphilic polymer-grafted graphene from polystyrene and polyacrylamide macroinitiators via radical coupling onto the vinyl bonds of GO.[29] On the basis of the functional groups of GO, both "grafting to" and "grafting from" strategies have been employed for polymer grafting. By direct esterification with GO and conversion of carboxyl groups into acyl chlorides, poly(vinyl alcohol) chains were grafted onto the surface of graphene via the grafting to strategy.[30] Through the "grafting from" strategy, vinyl polymers such as polystyrene and poly(methyl methacrylate) were successfully grafted on GO sheets via surface-initiated atom transfer radical polymerization.[22,31] Notably, all of the grafted polymers are almost vinyl polymers, whereas how to functionalize graphene or GO with polycondensation-type polymers is rarely investigated[32] and needed to be explored.

Herein, we first report an effective protocol to prepare nylon-6− (PA6−) graphene (NG) composites on the basis of carboxyl groups of GO by *in situ* polymerization with simultaneously thermal reduction to graphene from GO. Modified graphene sheets were homogenously dispersed in composites because of the high content of grafted PA6 arms on graphene sheets up to 78 wt %. Moreover, we prepared meter-long NG fibers by melt-spinning process, and found that both the tensile strength and Young's modulus of fibers are dramatically increased with only 0.1 wt % graphene loading.

Experimental Section

Materials. Graphite powder (40 μm) was obtained from Qingdao Henglide Graphite Co., Ltd. Concentrated H_2SO_4 (98%), $KMnO_4$, caprolactam, and 6-aminocaproic acid were purchased from Shanghai Reagents Company and used as received.

Characterization. Atomic force microscopy (AFM) images of GO and nylon-6-grafted graphene sheets were taken in the tapping mode by carrying out on Nano Scope III A and NSK SPI3800 respectively, with samples prepared by spin-coating sample solutions onto freshly exfoliated mica substrates at 1000 rpm. Scanning electron microscopy (SEM) images were taken on a Hitachi S4800 field-emission SEM system. X-ray photoelectron spectroscopy (XPS) was recorded on a PHI 5000c ESCA photoelectron spectrometer. X-ray diffraction (XRD) measurements were performed on a Philips X'Pert PRO diffractometer equipped with Cu Kα radiation (40 kV, 40 mA). Raman spectra were collected on a Jobin-Yvon LabRam HRUV Raman spectroscope equipped with a 514.5 nm laser source. Fourier-transform infrared (FT-IR) spectra were recorded on a Bruker Vector 22 spectrometer (KBr disk). Differential scanning calorimetric (DSC) analysis was performed on a Mettler TAGS equipment. In DSC analysis, dried samples under vacuum were heated to 100 °C and cooled slowly to room temperature in the first cycle to remove thermal history. The data were collected using a heating rate of 20 °C/min in a nitrogen atmosphere in the second cycle. Thermal gravimetric analysis (TGA) was done in a TGA PYRIS6 equipment from PE, using a heating rate of 20 °C/min in a nitrogen atmosphere. The stress−strain curves of single fiber were collected under a draw speed of 5 cm/min at room temperature. To get the intrinsic viscosity (η_{in}) of free PA6, the viscosity measurements were took in 85% formic acid solution of nylon-6 with a concentration of 5 g/L, in an Ubbelohde viscometer at 30 °C.

Synthesis of Graphene Oxide. GO single sheets were synthesized from natural graphite powder using a modified Hummers' method;[24,33] the synthesis procedure consisted of two steps of oxidation. In the preoxidation step, concentrated H_2SO_4 (40 mL) was put into a 500 mL round-bottom flask and heated to 80 °C. $K_2S_2O_8$ (8.4 g) and P_2O_5 (8.4 g) were added successively, followed by slow addition of graphite powder (10 g). The mixture was kept at 80 °C for 4.5 h. After cooling down to room temperature, the mixture was diluted with deionized water and left overnight. Then the mixture was vacuum-filtered and washed with deionized water (1.6 L) using a 0.22 μm polycarbonate membrane. The solid was dried in air at room temperature. In the second oxidation step, a 1.5 L three-necked round-bottom flask containing 230 mL of concentrated H_2SO_4 was chilled to 0 °C. The preoxidized sample was added into the flask and stirred. Then, $KMnO_4$ (60 g) was added slowly under continuous stirring, and the temperature was kept below 10 °C. The mixture was heated to 35 °C and stirred for 2 h. The mixture was then diluted with deionized water (0.5 L) and stirred for 2 h. Successively, additional 1.5 L of deionized water was added, followed by dropwise adding of 30% H_2O_2 (25 mL). The mixture was left undisturbed for 4 days and the nearly clear supernatant was decanted. The precipitate mixture was repeated water-washing and centrifugation successively with 1 M HCl solution at least three centrifugation cycles to remove residual metal oxides and with deionized water until the decantate became neutral. At last, GO dispersion in water was sonicated for 30 min. After centrifugation, the brown mixture was vacuum-dried under P_2O_5 at room temperature for 5 days.

Preparation of Nylon-6-Graphene (NG) Composites. A typical procedure to prepare graphene−nylon 6 composites with 0.1 wt % containing was depicted as follows: GO (10 mg) and caprolactam (9 g) were loaded into a 50 mL three-neck round-bottom flask and the mixture was sonicated at 80 °C for 2 h to obtain a homogeneous brown solution of GO, followed by introducing aminocaproic acid (1 g). After equipped a mechanical stirring and a N_2 inlet, the mixture was heated at 180 °C for 1 h at 250 °C for 9 h with a steady stirring. The color changed gradually from brown to black and the viscosity was also gradually enhanced during the reaction. After cooling to room temperature, the hard bulk was chopped into small pieces and washed in boiling water for 5 h by three times to remove monomer and low molecular weight oligomers completely. The washed black pieces of NG composites were dried at 80 °C in vacuum for 24 h. In the end, we obtained NG composites noted as NG-0.01, NG-0.1, NG-0.5, NG-1, NG-5, and NG-10, according to the feed weight percentage of GO. Through repeating centrifugal-washing by formic acid to remove free PA6, purified PA6-grafted graphene (PNG) brushes were obtained. The free PA6 was also collected by precipitation into methanol.

Melt-Spinning Process for NG Composites Fibers. The fibers of composites were fabricated using a self-made apparatus. The composite pieces in glass injector were heated to 250 °C for 10 min under N_2 atmosphere and the composite melt was pressed with N_2 (1 MPa) to extrude through the pinhole to form several meters long continuous fiber when cooled in the ambient atmosphere. The continuous fibers were enwound on a steadily rotating roll.

Results and Discussion

Synthesis of Nylon-6−Graphene Composites. Nylon, a kind of well-known condensation-type polymer, shows extensive applications in the field of fibers and engineering

Scheme 1. Synthesis of NG Composites by *in situ* Ring-Opening Polymerization of Caprolactam in the Presence of GO[a]

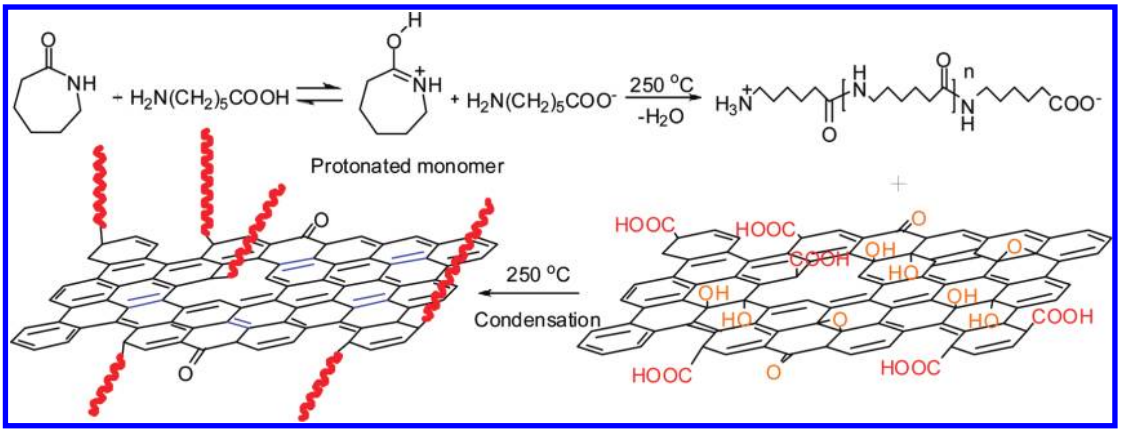

[a] The blue bonds in the nylon 6-grafted graphene represent restored conjugated bonds through high-temperature reduction; the red curves represent the grafted PA6 macromolecular chains.

materials. Previously, nylon/CNTs composites have been fabricated and exhibited enhanced mechanical properties.[34−36] Considering the totally different topology between CNTs and graphene, how to prepare fine nylon/graphene composites and their properties ripe for investigation. In our experiments, NG composites with a range of graphene loadings were synthesized by *in situ* ring-opening polymerization of caprolatam in the presence of GO, initiated by 6-aminocaproic acid (Scheme 1). The homogeneous dispersion of graphene in the resultant NG composites requires good dispersion of precursors (GO) in melt monomers (caprolatam). Besides providing grafting points to polymer functionalization, the pendent functional groups on GO platelets also offer strong interaction with polar organic solvents[37] and monomers, rendering homogeneous dispersion of GO in the mixture of melting caprolatam and 6-aminocaproic acid after sufficient sonication treatment. In addition, the homogeneous dispersion of GO avoids using solvents and excludes possible aggregation caused by solvent evaporation.

At elevated temperature, caprolactam was initiated by 6-aminocaproic acid and polymeric chains of PA6 step-propagated along with the consumption of monomers. Synchronously, part of the active PA6 chains were immobilized onto the sheets, by condensation reaction between the carboxyl acid groups of GO with active amino groups at PA6 chains terminals, having analogous grafting mechanism to the preparation of carbon nanotube (CNT)-based polyamides composites from functionalized CNTs.[34−36] Along with continuous propagation of polymer chains, the viscosity of the mixture increased gradually and the melting NG composites with lower feed ratio of GO than 1 wt % obviously exhibited Weissenberg effect[38] under stable stirring at the end of reaction, indicating the high molecular weight of PA6 we synthesized. Moreover, the color of melting mixture turned from brown to black (Figure 1a), suggesting restoration of conjugated planes for the thermal reduction of GO to graphene by decomposition of labile oxygen-contained moieties such as epoxy and hydroxyl groups.[26,27]

In the process of condensation polymerization, the excessive carboxylic acid groups on GO sheets inevitably disrupt the stoichiometric balance between carboxylic acids and amino groups in reaction system, by grafting polymer chains onto graphene sheets and simultaneously terminating potential propagation of active chains ends. Thus, the higher feed ratio of GO to monomer and the more content of carboxylic acids of GO mean the smaller molecular weight of grafted polymer chains corresponding to the less weight fraction of grafted polymer. Deduced from the condensation polymerization theory by Flory,[39] we deduced the inverse function relationship between the degree of polymerization (X_n) and the weight percentage of GO (w_{GO}), representing in eq 1 (the deduction of eq 1 see SI).

$$X_n = k w_{GO}^{-1} \quad (1)$$

Structure and Properties of PNG 2D Brushes. GO sheets perform soluble in water and DMF[37] but insoluble in the good solvents of PA6 such as formic acid, concentrated sulfuric acid, and *m*-cresol. The thermal reduced GO (RGO) prepared by annealing at 250 °C for 10 h are insoluble in all the aforementioned solvents, even after long-time sonication. After successful grafting, the covalently grafted chains of PA6 change the surface properties of graphene sheets and impact good solubility to the modified graphene in the good solvents of PA6. As shown in Figure 1b, both of the resultant NG composites and PNG sheets are dissolved homogenously in formic acid, concentrated sulfuric acid and *m*-cresol, without aggregation of graphene sheets for half a year, implying the high efficiency of polymer grafting. To affirm the uniform grafting effect on the graphene sheets, we took AFM measurement, the most used method to validate the structure of modified single graphene sheet with size in microscale, to visualize the PNG single sheets deposited by spin-casting from its formic acid solution. Figure 1c and Figure 1, parts d and e show the tapping mode AFM images of GO and PNG sheets, respectively. The grafted chains on two sides of graphene sheets heighten its thickness to about 8 nm, comparing to the thickness of GO about 0.8 nm. Moreover, the grafted PA6 chains cover the whole plane of graphene with even height (Figure 1d,e), suggesting the high density of grafting with a fabulous efficiency. Interestingly, such PA6-grafted graphene nanosheets represent a novel kind of 2D macromolecular brushes, which is hoped to be applied as building blocks for facile fabrication of large-area surface brushes used in the lubrication-related systems and other nanotechnology.[40]

To further validate the very existence of grafted PA6 chains on graphene sheets, we used XPS to characterize GO and PNG-0.5, as shown in Figure 2. In the XPS spectrum of GO, two obvious peaks are observed at 288.0 eV (C 1s) and 534.0 (O 1s), and no peak of nitrogen element was detected. For the sample PNG-0.5, strong signal of N 1s was found at 401.0 eV besides the signals of C 1s and O 1s,

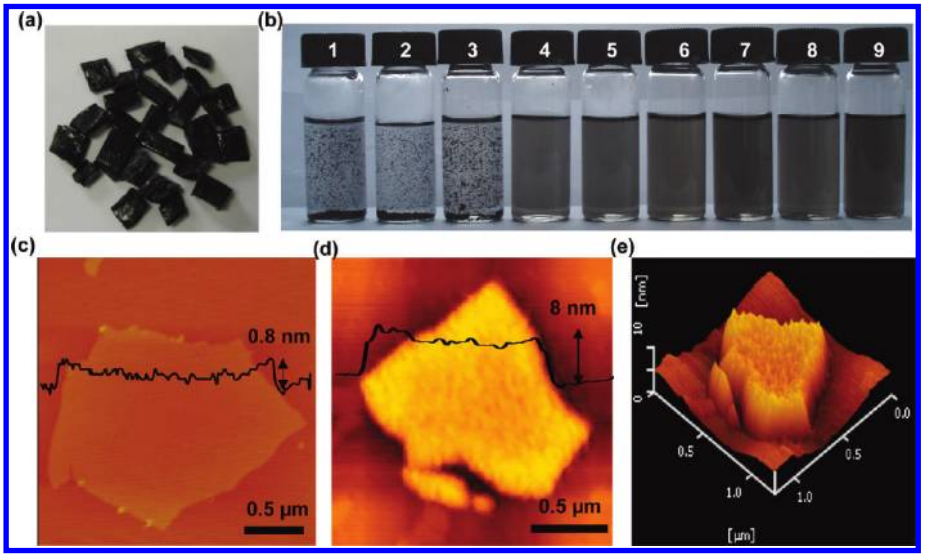

Figure 1. (a) Pieces of chopped NG-0.5 composites. (b) Reduced GO (1, 2, 3), NG-0.5 (4, 5, 6), and PNG-0.5 (7, 8, 9) dispersed in sulfuric acid, formic acid, and *m*-cresol, respectively. (c) AFM height image of GO on mica deposited from aqueous solution. (d) AFM height image, and (e) 3D-view image of purified nylon-grafted graphene brushes (PNG-0.5) on mica spinning-cast from the solution of formic acid.

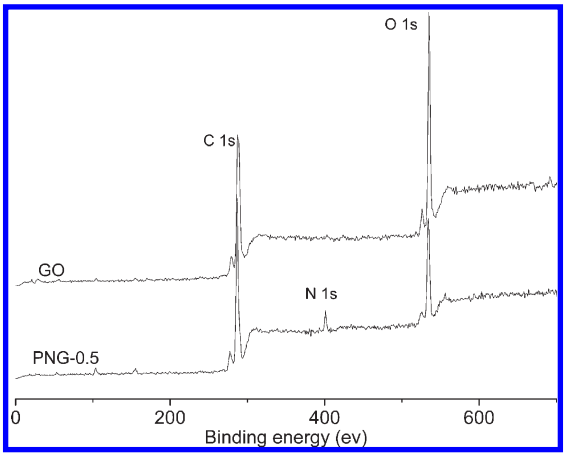

Figure 2. XPS spectra of GO and PNG-0.5. The peaks located at 401.0 and 534.0 eV denote the nitrogen and oxygen elements, respectively.

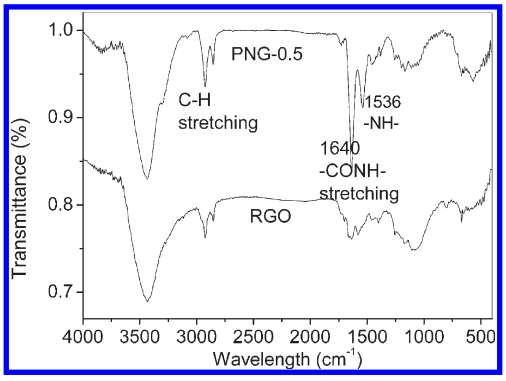

Figure 3. FTIR spectra of thermally reduced GO (RGO) and PNG-0.5.

indicating the abundance of nitrogen element in PA6-grafted graphene sheets.[41] The relative atomic concentration ratio of nitrogen to carbon (N/C) in PNG-0.5 is 0.069, close to the calculated value (0.08) from the corresponding TGA results (78 wt % of grafted nylon-6 and 22 wt % graphene). These results confirmed the successful grafting PA6 chains onto the graphene sheets. Moreover, we also detected characteristic bands of PA6 in the FTIR spectrum of PNG sheets without free PA6 chains (Figure 3), compared with that of thermally reduced GO at 250 °C for 10 h: the new emerged broad band at 1640 cm^{-1} corresponds to the stretching vibration of the C═O groups of the amide functionality; another new band at 1536 cm^{-1} is assigned to the bending vibration of the N−H bond and the stretching vibration of the C−N bond of the amide groups; the stronger bands at 2860 and 2930 cm^{-1} are due to the C−H stretching vibrations of grafted PA6 chains. All these results undoubtedly indicated the existence of PA6 chains grafted on graphene.

Theoretical deduction of condensation polymerization concluded that the molecular weight of free polymer and quantity of grafted polymer on graphene sheets decreased with the introduction of precursor of graphene (eq 1). Figure 4a shows the TGA curves of GO and PNG sheets in which the free polymers had been removed completely. The weight loss below 150 °C is due to the release of water contained in GO samples. It is found that the main weight loss of GO (about 35%) occurred below 250 °C (the onset temperature is 220 °C), assigning to the decomposition of the oxygen-contained functional moieties such as epoxy and hydroxyl that were introduced onto GO sheets during the oxidation of graphite.[27] On the contrary, the PNGs kept thermal stability up to 350 °C (the onset temperature is 382 °C) and no weight loss was detected below 250 °C, suggesting that the unreacted labile functional groups of GO material had been degraded into conjugated bonds or decomposed during the high-temperature polycondensation. Accordingly, the GO material has been thermally reduced into graphene simultaneously with the grafting of PA6 chains in such a one-pot in situ polymerization, giving rise to PA6-grafted graphene brushes. The weight loss values of grafted PA6 below 550 °C, the quantities of grafted PA6 on graphene sheets, are found to be 78%, 63.5%, 58% and 31%, for PNG-0.5, PNG-1.0, PNG-5.0, and PNG-10.0, respectively, indicating that the grafted polymer content decreases with increasing feed fraction of GO.

To speculate the length of grafted PA6 chains on graphene sheets, we investigated the molecular weight of free PA6 collected from the supernate of NG composites solution after centrifuging. The intrinsic viscosity (η_{in}) of free PA6 was obtained from the viscosity measurements in 85%

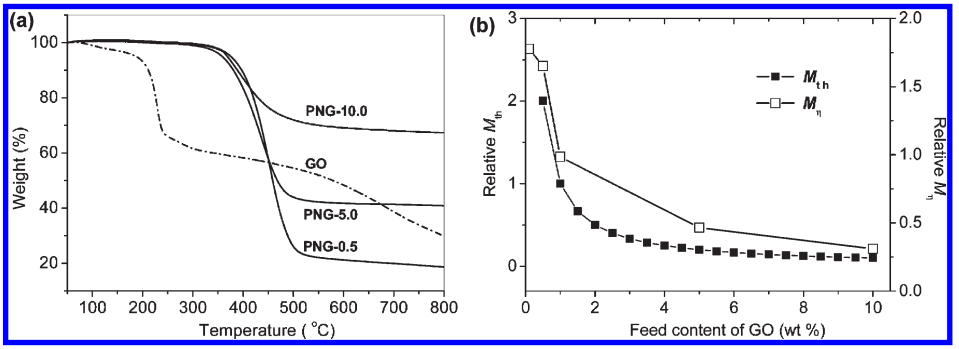

Figure 4. (a) TGA curves of the pristine GO and PNG sheets. (b) The measured viscosity-average molecular weight (M_η) of free nylon-6 (blank rectangle) and theoretically deduced molecular weight (M_{th}) from eq 1 (filled rectangle) as a function of feed content of GO.

Table 1. Molecular Weight of Free Nylon 6 and Thermal Properties of NG Composites

samples	PA6	NG-0.01	NG-0.1	NG-0.5	NG-1.0	NG-5.0	NG-10.0
$[\eta]^a$	0.78	0.74	0.69	0.65	0.425	0.23	0.165
$M_\eta{}^b$	20 636	19 350	17 769	16 521	9840	4654	3103
W_{550} °C^c	3.0	5.2	3.6	4.5	8.5	15.8	27.7
T_m (°C)^d	218.6	218.6	219.2	218.2	217.3	206	201.2

[a] Intrinsic viscosity of free nylon-6 of NG composites, which was measured at 25 °C in 85% formic acid solution by a Ubbelohde viscometer. [b] The molecular weight of free PA6 thereof was calculated from Mark−Houwink equation, where $K = 2.26 \times 10^{-4}$ and $\alpha = 0.82$.[42] [c] The residual weight percentage at 550 °C in the corresponding TGA curve. [d] The melting temperature measured by DSC.

formic acid solution in a Ubbelohde viscometer, and the viscosity-average molecular weight (M_η) was calculated from Mark−Houwink equation, $\eta_{in} = K[M_\eta]^\alpha$ (where $K = 2.26 \times 10^{-4}$ and $\alpha = 0.82$).[42] Table 1 shows that the molecular weights of free PA6 samples decreased with increasing the feed fraction of GO, from 20636 for neat PA6 to 3103 g/mol for NG-10 composite. Figure 4b gives the relationship between the measured M_η and the theoretic molecular weight (M_{th}) calculated from eq 1 with the feed percentage of GO, showing the similar decreasing tendency with increasing the feed content of GO. The result is also in accordance with the weight loss data of TGA shown in Figure 4a, that is the amount of PA6 grafted on graphene decreased with increasing the feed content of GO. The similar conclusions were obtained during *in situ* condensation polymerization of CNT-based PA6 composites from acidified carbon nanotubes[34] and CNT-grafted polyurea from amino-functionalized CNTs.[43] We believe that the general theoretical deduction on grafting polymerization to nanoparticles will render more reasonable design of graphene-based composites in the future.

Characterization and Thermal Properties of NG Composites. The presence of thermally reduced graphene in NG composites was confirmed by TGA curves (Figure 5) and Raman spectroscopy (Figure 6) of NG composites. TGA results of NG composites reveal the existence of graphene in the resultant NG composites (Figure 5 and Table 1). The residual weight percentages above 550 °C indicate the amount of graphene in composites and increased with the feed content of GO. Furthermore, the NG composites with graphene containing lower than 1.0 wt % are stable before 380 °C, revealing the thermal reduction of GO into graphene and good thermal stability of the NG composites. It is obviously detected that NG-10.0 performs lower temperature of decomposition threshold in TGA test (350 °C), suggesting the low molecular weight of PA6 in the composite for the intense disruption to stoichiometric balance caused by excessive carboxylic acids of GO.

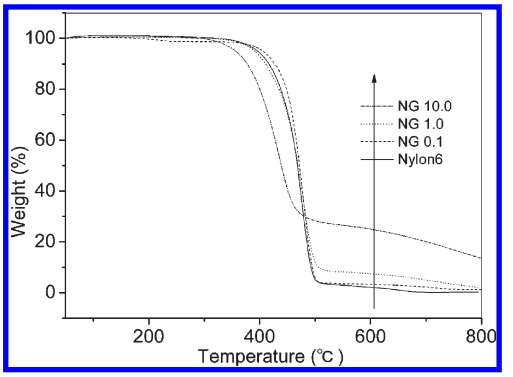

Figure 5. TGA curves of NG composites. The arrow directs the sequence of the curves from bottom to up.

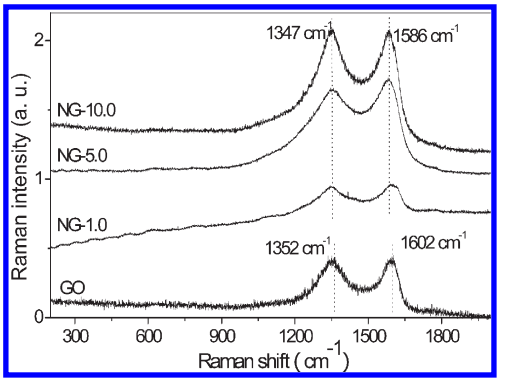

Figure 6. Raman spectra of NG composites.

The Raman spectra in Figure 6 show the characteristic peaks located at 1347 and 1586 cm^{-1} corresponding to the *D* and *G* bands of graphene sheets respectively,[44] and the intensity of the two peaks scales up with the content of graphene in composites, which is consistent with the results from TGA tests of NG composites. Referring to the *G* band of GO (1602 cm^{-1}), the *G* band of NG composites (1586 cm^{-1}) shifts toward lower wavelength which close to the value of graphite, further bearing out the thermal reduction of GO during condensation polymerization. Therefore, we could conclude that the *in situ* condensation as a protocol to fabricate nanocomposites from GO offers dual advantages including effective grafting and thermal reduction of GO, which is valuable for the composites for electric resistance application.

In composites of crystalline polymer, the crystallization impacts great influences to their performances. Therefore, investigation to the crystallization of graphene-based composites is

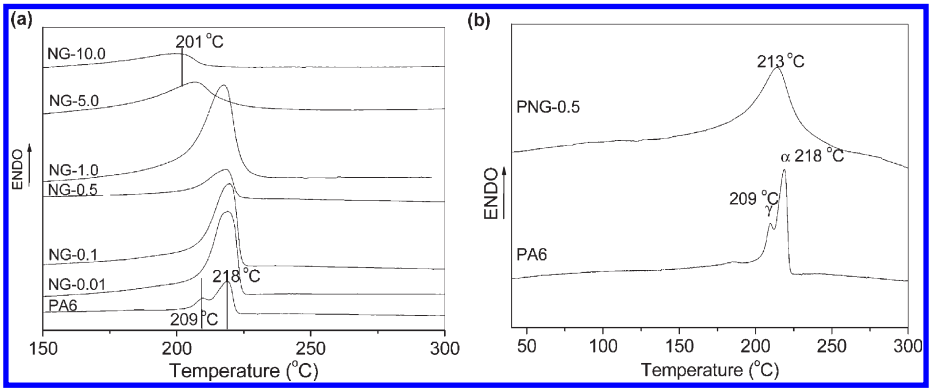

Figure 7. DSC curves of NG composites (a) and free PA6 and PA6-grafted graphene of PNG-0.5 (b).

needed to deeply understand the dispersion behavior of graphene sheets in crystalline polymers. In NG composites, the well-dispersed graphene sheets block off the interconnected matrices to form confined regions of PA6 chains. The more containing of graphene means intenser confinements to PA6 chains. It is well-known that PA6 has two crystal forms at least: more thermodynamically stable α-form crystal with hydrogen bonds between antiparallel chains and γ-form crystal with hydrogen bonds between parallel chains, indicated by T_m peaks at 218 and 209 °C in DSC curves, respectively.[45] As shown in DSC curves of NG composites (Figure 7a and Table 1), T_m peak at 209 °C disappears on the introduction of graphene into the composites, suggesting the depressed γ-form crystal of PA6 by well-dispersed graphene sheets. With increasing the graphene loading, T_m peak of α-form crystal at 218 °C becomes broader and weaker, indicating the incomplete α-form crystals for the confined mobility of polymer chains, which is a leading dynamic factor to form crystals by arrangements of polymer chains. Moreover, T_m peak at 218 °C moves to lower temperatures with increasing graphene content, answering for that the molecular weight of the polymer decreases with increasing GO content for the termination to the active chains by carboxyl acids on GO sheets during the *in situ* polymerization for NG composites. From the DSC curves of free PA6 and PNG brushes in Figure 7b, we also find that PNG-0.5 has a wider and lower T_m peak at 213 °C, implying the depressed crystallization behavior of PA6 chains anchored on the graphene sheets. Further evidence for depressed crystallization in NG composites are demonstrated by their XRD patterns (Figure 8). The diffraction peaks located at 2θ 20° and 24° are corresponding to (200) and (002, 220) reflections in α-form crystals of PA6, respectively.[45] Along the increasing containing of graphene, the diffraction peaks of α-form crystals become weaker, confirming the depressed crystallization in NG composites. These results declared that 2D nanosheets have significant influence on the crystallization, aggregation or assembly behaviors of polymer chains.

Graphene Dispersion in NG Composites and Its Reinforcement to NG Fibers. Resulted from the successful grafting on graphene by PA6 chains, the modified surface characteristics rendered homogeneous dispersion of functionalized graphene sheets in NG composites, revealed by SEM images of NG cross-section composites (Figure 9a,b). The bright regions are attributed to the graphene sheets for their high conductivity. It is obviously inspected that the bright regions are well-distributed in PA6 matrix (dark region) without congregation. We could inspect the typical stretched and wrapped patterns of graphene sheets in the spaced PA6 regions. As shown by the SEM images of neat PNG sheets in Figure 9c,d, the polymer-grafted sheets are curl-folded together, performing bright edges with uniformly narrow

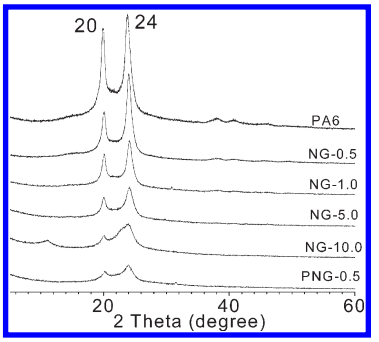

Figure 8. XRD patterns of NG composites and PNG-0.5.

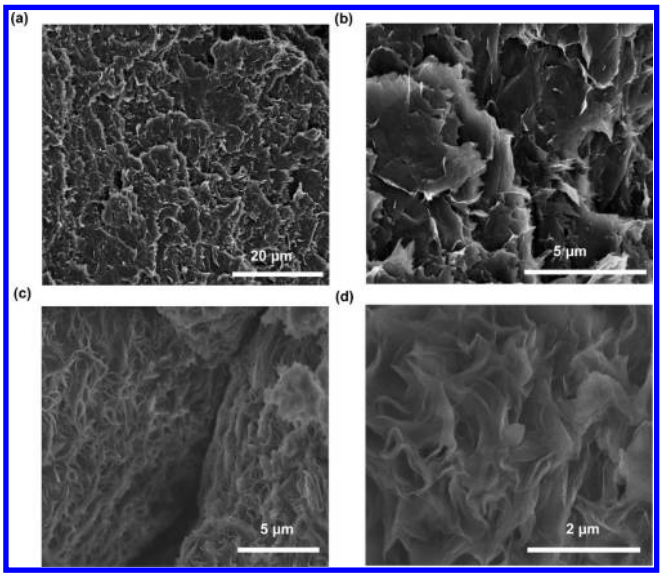

Figure 9. SEM images of cross-section from NG-0.5 composites (a, b) and bulk PNG-0.5 (c, d).

thickness. The homogeneous dispersion of graphene is ascribed to the high density of grafting, which enhanced the interfacial interaction with matrix. It is also attributed to the *in situ* polymerization protocol, in which graphene sheets are kept homogeneously along polymerization of the intercalated caprolactam monomers between layers. The resultant homogeneous dispersion of graphene sheets in composites by *in situ* polymerization provides the utmost element to obtain superior performances of nanocomposites.

Graphene sheets have been applied to reinforce the composites from both aspects of theory[46] and experiments.[22,23] From aforementioned investigations to NG composites, the

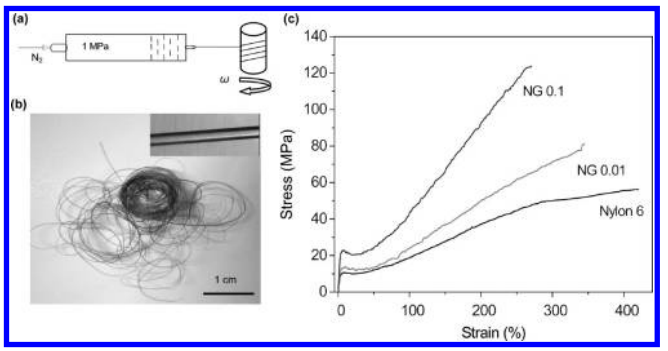

Figure 10. (a) Apparatus of melt spinning for NG composites fibers, the dot line indicated the melt NG composites at 250 °C. (b) Photograph of NG-0.5 fibers, the inset showed the diameter of the fiber was about 50 μm under an optical microscope. (c) Stress−strain curves of neat PA6 and NG composite fibers with 0.01 and 0.1 wt % loading of graphene.

homogeneous dispersion of graphene nanosheets in PA6 matrix would result in potential reinforcement for the effective loading transference, especially at low containing of graphene. To evaluate the strengthening effect of graphene, we processed NG composites to continuous fibers by melt-spinning process, of which the apparatus is illustrated in Figure 10a. The diameter of fibers fabricated in our process was about 50 μm and performed homogeneous without aggregation of graphene sheets in fibers. As shown in Figure 10b, the fibers under microscope show smooth surface. The mechanical properties of NG composites fibers are illustrated in Figure 10c. At low containing of graphene, NG fibers show distinct yield points for crystalline polymer, probably for the orientation-induced crystallization at high draw ratio. Pure PA6 fiber performs a tensile strength of 56 MPa and a break elongation of 420%, a little stronger than pure nylon films[47] for the axis drawing orientation. The fiber of 0.01 wt % graphene containing has a tensile strength of 84 MPa, which is higher than that of nylon fiber by 50%, and performs a lower break elongation of 343%. When the graphene containing increases up to 0.1 wt %, the tensile strength is dramatically enhanced up to 123 MPa (2.2 folds over that of PA6 fiber), companying with further decreasing of break elongation at 269%. Increasing with the containing of graphene, the Young's modulus increases from 305 MPa for neat PA6 to 722 MPa for NG-0.1 fiber. Undoubtedly, the excellent reinforcement of graphene could be attributed to the good dispersion of graphene sheets in composites and the strong interaction between the PA6-grafted graphene and PA6 matrix.

Besides condensation polymerization to prepare nylon-6 composites, anionic polymerization promises the preparation of graphene-based nanocomposites more swiftly, which was proven effective in the fabrication of nylon-6 composites of carbon nanotubes,[48] clay,[49] and other polymer matrices,[50] being our works in process. Notably, as a kind of nanofiller with asymmetric shapes, graphene with oriented arrangement in composites could promises greater enhancements to the mechanical properties, companying with improvements by chemical engineering of graphene-PA6 interface and uniformalization of the sizes of graphene sheets. Further investigations on mechanical improvement of NG composites and preparation to other graphene−based condensation polymer composites by *in situ* protocol are in progress.

Conclusions

We prepared graphene−PA6 composites by *in situ* ring-opening polymerization of caprolactam in the presence of graphene oxide (GO). By a condensation reaction between the carboxylic acid groups on GO and terminal amino ends of PA6 chains, the macromolecular chains of PA6 were effectively grafted onto GO sheets, accompanying with the reduction from GO to graphene. The grafted graphene sheets showed good solubility in the good solvents of PA6 and performed good compatibility to PA6 matrix in composite. With enhanced interfacial interaction to the matrix, the modified graphene impacted great reinforcements to PA6 fibers as made by melt spinning. The Young's modulus and tensile strength of NG composite fibers were greatly improved even though at very low containing of graphene, offering great promises for wider application of PA6 materials. The *in situ* condensation polymerization we brought opens a new avenue to fabricate graphene-based nanocomposites of condensation polymers scalably and effectively for more extensive applications.

Acknowledgment. This work was financially supported by the National Natural Science Foundation of China (No. 50773038 and No. 20974093), National Basic Research Program of China (973 Program) (No. 2007CB936000), the Fundamental Research Funds for the Central Universities (No. 2009QNA-4040), and the Foundation for the Author of National Excellent Doctoral Dissertation of China (No. 200527). Thanks are expressed for the help from Prof. Jinwen Qian in the measurements of intrinsic viscosity.

Supporting Information Available: Text giving the theoretical calculation of the basic equation. This material is available free of charge via the Internet at http://pubs.acs.org.

References and Notes

(1) Kroto, H. W.; Hwath, S. C.; O'Brien, R. F. C.; Smalley, R. E. *Nature* **1985**, *318*, 162–163.
(2) Iijima, S.; Ichihashi, T. *Nature* **1993**, *336*, 603–605.
(3) Novoselov, K. S.; Geim, A. K.; Morozov, S. V.; Jiang, D.; Katsnelson, M. I.; Grigorieva, I. V.; Dubonos, S. V.; Firsov, A. A. *Nature* **2004**, *438*, 197–200.
(4) Geim, A. K.; Novoselov, K. S. *Nat. Mater.* **2007**, *6*, 183–191.
(5) (a) Hu, Y. H.; Shenderova, O. A.; Hu, Z. S.; Padgett, C. W.; Brenner, D. W. *Rep. Prog. Phys.* **2006**, *69*, 1847–1895. (b) Thompson, B. C.; Fréchet, J. M. J. *Angew. Chem., Int. Ed.* **2007**, *47*, 58–77. (c) Moniruzzaman, M.; Winey, K. I. *Macromolecules* **2006**, *39*, 5194–5205. (d) Coleman, J. N.; Khan, U.; Gun'ko, Y. K. *Adv. Mater.* **2006**, *18*, 689–706. (e) Jang, B. Z.; Zhamu, A. *J. Mater. Sci.* **2008**, *43*, 5092–5101.
(6) (a) Qian, D.; Dickey, E. C.; Andrews, R.; Rantell, T. *Appl. Phys. Lett.* **2000**, *76*, 2868–2870. (b) Sabba, Y.; Thomas, E. L. *Macromolecules* **2004**, *37*, 4815–4820. (c) Liu, T. X.; Phang, I. Y.; Shen, L.; Chow, S. Y.; Zhang, W. D. *Macromolecules* **2004**, *37*, 7214–7222. (d) Zhang, Z. N.; Zhang, J.; Chen, P.; Zhang, B. Q.; He, J. S.; Hu, G. H. *Carbon* **2006**, *44*, 692–698.
(7) (a) Viswanathan, G.; Chakraoani, N.; Yang, H. C.; Wei, B. Q.; Chung, H. S.; Cho, K. W.; Ryu, C. Y.; Ajayan, P. M. *J. Am. Chem. Soc.* **2003**, *125*, 9258–9259. (b) Kong, H.; Gao, C.; Yan, D. Y. *J. Am. Chem. Soc.* **2004**, *126*, 412–413. (c) Qu, L. W.; Lin, Y.; Hill, D. E.; Zhou, B.; Wang, W.; Sun, X. F.; Kitaygorodskiy, A.; Suarez, M.; Connell, J. W.; Allard, L. F.; Sun, Y. P. *Macromolecules* **2004**, *37*, 6055–6060. (d) Lin, Y.; Zhou, B.; Fernando, K. A. S.; Liu, P.; Allard, L. F.; Sun, Y. P. *Macromolecules* **2003**, *36*, 7199–7204. (e) Qin, S. H.; Qin, D. Q.; Ford, W. T.; Herrera, J. E.; Resasco, D. E. *Macromolecules* **2004**, *37*, 9963–9967. (f) Xu, Y. Y.; Gao, C.; Kong, H.; Yan, D. Y.; Jin, Y. Z.; Watts, P. C. P. *Macromolecules* **2004**, *37*, 8846–8853.
(8) Tasis, D.; Tagmatarchis, N.; Bianco, A.; Prato, M. *Chem. Rev.* **2006**, *106*, 1105–1136.
(9) (a) Chen, G. H.; Wu, D. J.; Weng, W. G.; Yan, W. *Polym. Eng. Sci.* **2001**, *41*, 2148–2154. (b) Chen, G. H.; Wu, D. J.; Wu, C. *Carbon* **2003**, *41*, 619–621. (c) Pan, Y. X.; Yu, Z. Z.; Ou, Y. C.; Hu, G. H. *J. Polym. Sci., Part B: Polym. Phys.* **2000**, *38*, 1626–1633. (d) Chung, D. D. L. *J. Mater. Sci.* **1987**, *22*, 4190–4198.
(10) Stankovich, S.; Dikin, D. A.; Dommett, G. H. B.; Kohlhaas, K. M.; Zimney, E. J.; Stach, E. A.; Piner, R. D.; Nguyen, S. T.; Ruoff, R. S. *Nature* **2006**, *442*, 282–286.

(11) Bolotin, K. I.; Sikes, K. J.; Jiang, Z.; Klima, M.; Fudenberg, G.; Hone, J.; Kim, P.; Stormer, H. L. *Solid State Commun.* **2008**, *146*, 351–355.
(12) Zhang, Y.; Tan, Y. W.; Stormer, H. L.; Kim, P. *Nature* **2005**, *438*, 201–204.
(13) Lee, C.; Wei, X.; Kysar, J. W.; Hone, J. *Science* **2008**, *321*, 385–388.
(14) Balandin, A. A.; Ghosh, S.; Bao, W. Z.; Calizo, I.; Teweldebrhan, D.; Miao, F.; Lau, C. N. *Nano Lett.* **2008**, *8*, 902–907.
(15) Cai, D. Y.; Yusoh, K.; Song, M. *Nanotechnology* **2009**, *20*, 085712.
(16) (a) Watcharotone, S.; Dikin, D. A.; Stankovich, S.; Piner, R.; Jung, I.; Dommett, G. H. B.; Evmenenko, G.; Wu, S. E.; Chen, S. F.; Liu, C. P.; Nguyen, S. T.; Ruoff, R. S. *Nano Lett.* **2007**, *7*, 1888–1892. (b) Eda, G.; Chhowalla, M. *Nano Lett.* **2009**, *9*, 814–818. (c) Ansari, S.; Giannelis, E. P. *J. Polym. Sci., Part B: Polym. Phys.* **2009**, *47*, 888–897. (d) Zhang, H. B.; Zheng, W. G.; Yan, Q.; Yang, Y.; Wang, J. W.; Lu, Z. H.; Ji, G. Y.; Yu, Z. Z. *Polymer* **2010**, *51*, 1191–1196. (f) Cote, L. J.; Cruz-Silva, R.; Huang, J. X. *J. Am. Chem. Soc.* **2009**, *131*, 11027–11032. (e) Stoller, M. D.; Park, S.; Zhu, Y.; An, J.; Ruoff, R. S. *Nano Lett.* **2008**, *8*, 3498–3502.
(17) (a) Wang, H.; Hao, Q.; Yang, X.; Lu, L.; Wang, X. *Eletrochem. Commun.* **2009**, *6*, 1158–1161. (b) Chen, S.; Zhu, J. W.; Wu, X. D.; Han, Q. F.; Wang, X. *ACS Nano* **2010**, *4*, 2822–2830. (c) Zhang, K.; Zhang, L. L.; Zhao, X. S.; Wu, J. S. *Chem. Mater.* **2010**, *22*, 1392–1401. (d) Wu, Q.; Xu, Y. X.; Yao, A. R.; Shi, G. Q. *ACS Nano* **2010**, *4*, 1963–1970.
(18) (a) Shan, C. S.; Yang, H. F.; Han, D. X.; Zhang, Q. X.; Ivaska, A.; Niu, L. *Biosens. Bioelectron.* **2010**, *25*, 1070–1074. (b) Bai, H.; Li, C.; Wang, X. L.; Shi, G. Q. *Chem. Commun.* **2010**, *46*, 2376–2378. (c) Li, J.; Guo, S. J.; Zhai, Y. M.; Wang, E. K. *Anal. Chim. Acta* **2009**, *649*, 196–201.
(19) Park, S.; Mohanty, N.; Suk, J. W.; Nagaraja, A.; An, J.; Piner, R. D.; Cai, W. W.; Dreyer, D. R.; Berry, V.; Ruoff, R. S. *Adv. Mater.* **2010**, *22*, 1736–1740.
(20) Liang, M. H.; Zhi, L. J. *J. Mater. Chem.* **2009**, *19*, 5871–5878.
(21) (a) Zhang, H.; Bao, Q. L.; Tang, D. Y.; Zhao, L. M.; Loh, K. P. *Appl. Phys. Lett.* **2009**, *95*, 141103. (b) Sun, Z. P.; Hasan, T.; Torrisi, F.; Popa, D.; Privitera, G.; Wang, F. Q.; Bonaccorso, F.; Basko, D. M.; Ferrari, A. C. *ACS Nano* **2010**, *4*, 803–810.
(22) Fang, M.; Wang, K. G.; Lu, H. B.; Yang, Y. L.; Nutt, S. *J. Mater. Chem.* **2009**, *19*, 7098–7105.
(23) (a) Ramanathan, T.; Abdala, A. A.; Stankovich, S.; Dilin, D. A.; Herrear-Alonso, M.; Piner, R. D.; Adamson, D. H.; Schniepp, H. C.; Chen, X.; Ruoff, R. S.; Nguyen, S. T.; Aksay, I. A.; Prud'Homme, R. K.; Brinson, L. C. *Nat. Nanotechnol.* **2008**, *3*, 327–331. (b) Xu, Y. X.; Hong, W. J.; Bai, H.; Li, C.; Shi, G. Q. *Carbon* **2009**, *47*, 3538–3543. (c) Liang, J. L.; Huang, Y.; Zhang, L.; Wang, Y.; Ma, Y. F.; Guo, T. Y.; Chen, Y. S. *Adv. Funct. Mater.* **2009**, *19*, 1–6.
(24) Hummers, W. S., Jr.; Offeman, R. E. *J. Am. Chem. Soc.* **1958**, *80*, 1339.
(25) Dreyer, D. R.; Park, S.; Bielawski, C. W.; Ruoff, R. S. *Chem. Soc. Rev.* **2010**, *39*, 228–240.
(26) (a) Lerf, A.; He, H.; Forster, M.; Klinowski, J. *J. Phys. Chem. B* **1998**, *102*, 4477–4482. (b) Cai, W. W.; Piner, R. D.; Stadermann, F. J.; Park, S.; Shaibat, M. A.; Ishii, Y.; Yang, D. X.; Velamakanni, A.; An, S. J.; Stoller, M.; An, J.; Chen, D. M.; Ruoff, R. S. *Science* **2008**, *26*, 1815–1817.
(27) Gao, W.; Alemany, L. B.; Ci, L.; Ajayan, P. M. *Nature Chem.* **2009**, *1*, 403–408.
(28) Stankovich, S.; Dikin, D. A.; Piner, R. D.; Kohlhaas, K. A.; Kleinhammes, A.; Jia, Y. Y.; Wu, Y.; Nguyen, S. T.; Ruoff, R. S. *Carbon* **2007**, *45*, 1558–1565.
(29) Shen, J. F.; Hu, Y. Z.; Li, C.; Qin, C.; Ye, M. X. *Small* **2009**, *1*, 82–85.
(30) Salavagione, H. J.; Gómez, M. A.; Martínez, G. *Macromolecules* **2009**, *42*, 6331–6334.
(31) Lee, S. H.; Dreyer, D. R.; An, J. H.; Velamakanni, A.; Piner, R. D.; Park, S.; Zhu, Y. W.; Kim, S. O.; Bielawski, C. W.; Ruoff, R. S. *Maromol. Rapid. Commun* **2010**, *31*, 281–288.
(32) (a) Wang, D. W.; Li, F.; Zhao, J. P.; Ren, W. C.; Tan, J.; Wu, Z. S.; Gentle, L.; Lu, G. Q.; Cheng, H. M. *ACS Nano* **2009**, *3*, 1745–1752. (b) Yan, J.; Wei, T.; Shao, B.; Fan, Z. J.; Qian, W. Z.; Zhang, M. L.; Wei, F. *Carbon* **2010**, *48*, 487–493.
(33) Kovtyukhova, N. I.; Ollivier, P. J.; Martin, B. R.; Mallouk, T. E.; Chizhik, S. A.; Buzaneva, E, V.; Gorchinskiy, A. D. *Chem. Mater.* **1999**, *11*, 771–778.
(34) (a) Gao, J. B.; Itkis, M. E.; Yu, A. P.; Bekyarova, E.; Zhao, B.; Haddon, R. C. *J. Am. Chem. Soc.* **2005**, *127*, 3847–3854. (b) Gao, J. B.; Zhao, B.; Itkis, M. E.; Bekyarova, E.; Hu, H.; Kranak, V.; Yu, A. P.; Haddon, R. C. *J. Am. Chem. Soc.* **2006**, *128*, 7492–7496.
(35) Zeng, H. L.; Gao, C.; Wang, Y. P.; Watts, Paul., C. P.; Kong, H.; Cui, X. W.; Yan, D. Y. *Polymer* **2006**, *47*, 113–122.
(36) Phang, I. Y.; Ma, J. H.; Shen, L.; Liu, T. X.; Zhang, W. D. *Polym. Int.* **2006**, *55*, 71–79.
(37) Paredes, J. I.; Villar-Rodil, S.; Martinez-Alonso, A.; Tascon, J. M. D. *Langmuir* **2008**, *24*, 10560–10564.
(38) Weissenberg, K. *Nature* **1947**, *159*, 310.
(39) Flory, P. J. *Principles of Polymer Chemistry*; Cornell University Press: New York, 1953.
(40) (a) Raviv, U.; Giasson, S.; Kampf, N.; Gohy, J. F.; Jérôme, R.; Klein, J. *Nature* **2003**, *425*, 163–165. (b) Klein, J. *Science* **2009**, *323*, 47–48.
(41) Zhang, Y.; He, H. K.; Gao, C.; Wu, J. Y. *Langmuir* **2009**, *25*, 5814–5824.
(42) Gechele, G. B.; Mattiussi, A. *Eur. Polym. J.* **1965**, *1*, 47–61.
(43) Gao, C.; Jin, Y. Z.; Kong, H.; Whitby-Raymond., L. D.; Acquah-Steve., F. A.; Chen, G. Y.; Qian, H. H.; Hartschuh, A.; Silva, S. R. P.; Henley, S.; Fearon, P.; Kroto, H. W.; Walton-David., R. M. *J. Phys. Chem. B* **2005**, *109*, 11925–11932.
(44) Nemanich, R. J.; Solin, S. A. *Phys. Rev. B* **1979**, *20*, 392–401.
(45) Medellin-Rodriguez, F. J.; Larios-Lopez, L.; Zapata-Espinoza, A.; Davalos-Montoya, O.; Phillips, P. J.; Lin, J. S. *Macromolecules* **2004**, *37*, 1799–1809.
(46) Rafiee, M. A.; Rafiee, J.; Wang, Z.; Song, H. H.; Yu, Z. Z.; Koratkar, N. *ACS Nano* **2009**, *3*, 3884–3890.
(47) Zhang, W. D.; Shen, L.; Phang, I. Y.; Liu, T. *Macromolecules* **2004**, *37*, 256–259.
(48) Qu, L. W.; Veca, L. M.; Lin, Y.; Kitaygorodskiy, A.; Chen, B. L.; Macall, A. M.; Connell, J. W.; Sun, Y. P. *Macromolecules* **2005**, *38*, 10328–10331.
(49) Yu, Z. Z.; Hu, G. H.; Varlet, J.; Dasari, A.; Mai, Y. W. *J. Polym. Sci., Part B: Polym. Phys.* **2005**, *43*, 1100–1112.
(50) Hu, G. H.; Li, H. X.; Feng, L. F. *Polymer* **2005**, *46*, 4562–4570.